NAVAL POSTGRADUATE SCHOOL
Monterey, California

THESIS

DEVELOPMENT OF EXPERIMENTAL FACILITY FOR ROLL-ON ROLL-OFF RAMP ISOLATION DYNAMICS

by

Richard A. Trevisan

June 2001

Thesis Advisor:	Joshua H. Gordis
Thesis Co-Advisor:	Fotis A. Papoulias

Approved for public release; distribution is unlimited

20010803 007

REPORT DOCUMENTATION PAGE

Form Approved OMB No. 0704-0188

Public reporting burden for this collection of information is estimated to average 1 hour per response, including the time for reviewing instruction, searching existing data sources, gathering and maintaining the data needed, and completing and reviewing the collection of information. Send comments regarding this burden estimate or any other aspect of this collection of information, including suggestions for reducing this burden, to Washington headquarters Services, Directorate for Information Operations and Reports, 1215 Jefferson Davis Highway, Suite 1204, Arlington, VA 22202-4302, and to the Office of Management and Budget, Paperwork Reduction Project (0704-0188) Washington DC 20503.

1. AGENCY USE ONLY *(Leave blank)*	2. REPORT DATE	3. REPORT TYPE AND DATES COVERED
	June 2001	Master's Thesis

4. TITLE AND SUBTITLE: Title (Mix case letters)
Development of Experimental Facility for Roll-on Roll-off Ramp Isolation Dynamics

5. FUNDING NUMBERS
N0016700WR00366

6. AUTHOR(S) Trevisan, Richard A.

7. PERFORMING ORGANIZATION NAME(S) AND ADDRESS(ES)
Naval Postgraduate School
Monterey, CA 93943-5000

8. PERFORMING ORGANIZATION REPORT NUMBER

9. SPONSORING / MONITORING AGENCY NAME(S) AND ADDRESS(ES)
NSWC, Carderock Division
9500 MacArthur Blvd
West Bethesda, MD 20817-5700

10. SPONSORING / MONITORING AGENCY REPORT NUMBER

11. SUPPLEMENTARY NOTES The views expressed in this thesis are those of the author and do not reflect the official policy or position of the Department of Defense or the U.S. Government.

12a. DISTRIBUTION / AVAILABILITY STATEMENT
Approved for public release; distribution is unlimited

12b. DISTRIBUTION CODE

13. ABSTRACT ***(maximum 200 words)***

It has been determined that a high stress state occurs in the Roll-on Roll-off (RORO) ship offload stern ramp during vehicle transfers in Sea State 3 conditions. Motion compensation systems (i.e. isolators) between the ramp and the barge (RRDF) are needed to minimize the high stress levels in the ramp. This thesis documents the design, analysis, and construction of a facility to evaluate the performance of candidate isolation systems to be used to minimize ramp stresses. The facility consists of a fabricated aluminum scale ramp model designed to mimic the structural dynamics of a full-scale ramp, a fabricated supporting structure and an actuator that simulates wave motion inputs to the barge-end of the isolator.

14. SUBJECT TERMS
Isolation, Roll-on, Roll-off, RORO, stern ramp

15. NUMBER OF PAGES 46

16. PRICE CODE

17. SECURITY CLASSIFICATION OF REPORT	18. SECURITY CLASSIFICATION OF THIS PAGE	19. SECURITY CLASSIFICATION OF ABSTRACT	20. LIMITATION OF ABSTRACT
Unclassified	Unclassified	Unclassified	UL

NSN 7540-01-280-5500

Standard Form 298 (Rev. 2-89)
Prescribed by ANSI Std. 239-18

THIS PAGE INTENTIONALLY LEFT BLANK

Approved for public release; distribution is unlimited

DEVELOPMENT OF EXPERIMENTAL FACILITY FOR ROLL-ON ROLL-OFF RAMP ISOLATION DYNAMICS

Richard A. Trevisan
Lieutenant, United States Navy
B.S., Marquette University, 1993

Submitted in partial fulfillment of the
requirements for the degree of

MASTER OF SCIENCE IN MECHANICAL ENGINEERING

from the

NAVAL POSTGRADUATE SCHOOL
June 2001

Author: _____
Richard A. Trevisan

Approved by: _____
Joshua H. Gordis, Thesis Advisor

_____
Fotis A. Papoulias, Co-Advisor

_____
Terry R. McNelley, Chairman
Department of Mechanical Engineering

THIS PAGE INTENTIONALLY LEFT BLANK

ABSTRACT

It has been determined that a high stress state occurs in the Roll-on Roll-off (RORO) ship offload stern ramp during vehicle transfers in Sea State 3 conditions. Motion compensation systems (i.e. isolators) between the ramp and the barge (RRDF) are needed to minimize the high stress levels in the ramp. This thesis documents the design, analysis, and construction of a facility to evaluate the performance of candidate isolation systems to be used to minimize ramp stresses. The facility consists of a fabricated aluminum scale ramp model designed to mimic the structural dynamics of a full-scale ramp, a fabricated supporting structure and an actuator that simulates wave motion inputs to the barge-end of the isolator.

THIS PAGE INTENTIONALLY LEFT BLANK

TABLE OF CONTENTS

THIS PAGE INTENTIONALLY LEFT BLANK

LIST OF FIGURES

THIS PAGE INTENTIONALLY LEFT BLANK

LIST OF TABLES

THIS PAGE INTENTIONALLY LEFT BLANK

ACKNOWLEDGMENTS

The author would like to acknowledge the financial support of NAVSEA, Carderock, Surface Warfare Center Division for allowing the purchase of the equipment used in this thesis.

Professors Gordis and Papoulias, it has been a pleasure to work for you. Thank you for your guidance and patience during this study.

Thank you to CDR McCoy and Pam Silva. Your support through not only my thesis work but for my personal dealings as well was greatly appreciated.

I would like to thank Frank Franzen , Jim Lefler for all their work during the manufacture of the testing facility and allowing me to "help out".

Thank you to Tom McCord for letting me bend your ear while working over the preliminary design and arranging Public Work support.

Mardo Blanco, you can lay a bead like no other. Thank you for all your help.

There are many more people around the Naval Postgraduate School, too numerous to name, that I would like to thank. You know who you are.

Thank you to Mr. And Mrs. Eugene Hester and Mr. And Mrs. Richard Trevisan Sr. Your support and encouragement throughout this work was greatly appreciated.

Thank you to my children, Ricky and Elizabeth. Monterey is supposed to be a place for sending time with your family. We did a lot of great things together. Thank you for understanding when I had to go back to work.

Finally, they say behind every good man is a great woman. Well, I am married to the greatest. Emily, thank you for putting up with the long hours, the long days and the long weeks. I could not have done this without you. I am proud to call you my wife.

THIS PAGE INTENTIONALLY LEFT BLANK

I. INTRODUCTION

A. BACKGROUND

Roll-on Roll-off (RORO) ships transfer cargo such as vehicles to ports around the world. These deep draft ships are large and can only access a limited number of ports due to their draft and size requirements. Their cargo must them be shipped via land transportation to other areas the ship cannot deliver to.

Normally, the RORO would enter a port that is protected from the sea environment by a sea wall or land mass. Once the RORO is moored, a large ramp folds down off the stern of the ship to the pier. The cargo is then driven off the ship, across the ramp, and onto a pier or barge. Now, to access more ports, the intention is to offload the RORO to a shallow draft barge (RRDF) at sea. The RRDF may then enter the port not originally accessible by the RORO.

Offloading will occur in a sea state condition up to sea state 3. At sea with no protection from wave interactions, a high stress state occurs in the RORO offload stern ramp due to the motions between the RORO and the RRDF. Motion compensation systems (i.e. isolators) between the ramp and the RRDF are needed to minimize the high stress levels in the ramp to prevent failure.

This thesis documents the design, analysis, and construction of a facility to evaluate the performance of candidate isolation systems to be used to minimize ramp stresses. It will also be used to validate Mathematical models of the candidate isolation systems for further refinements to the systems.

The facility consists of a fabricated aluminum scale ramp model designed to mimic the structural dynamics of a full-scale ramp, a fabricated supporting structure and an actuator that simulates wave motion inputs to the barge-end of the isolator.

B. OBJECTIVES

The objectives of this thesis are to design, analyze and manufacture the RORO ramp isolation dynamics facility, which will evaluate the performance and validate Mathematical models of candidate isolation systems to be used to minimize ramp stresses. All calculation equations and material specifications are taken from [Ref. 1] thru [Ref. 3].

II. THE EXPERIMENTAL FACILITY

A. THE SCALE RAMP MODEL

The ratio of the scale ramp model to the full size RORO ramp is 13:1. This ratio was chosen so the ramp would be small enough to suit a laboratory environment yet big enough that instrumentation placed on the ramp could obtain adequate data for analysis. The overall dimensions of the ramp model are 2 feet wide, 8 feet long, and 2 inches deep. Figure 1 shows an isometric view of the ramp model.

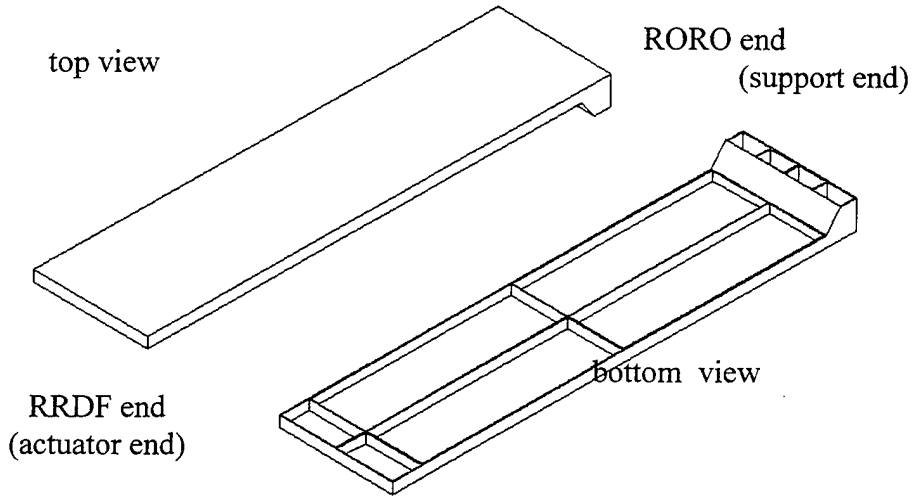

Figure 1. Ramp Model.

1. Construction and Fabrication

The ramp is entirely made up of quarter-inch thick aluminum plate except for the support end, which uses half-inch thick aluminum plate to facilitate mounting to the support structure. The top is one piece, 2 feet wide by 8 feet long. Three longitudinal stiffening ribs measuring 2-inch wide and 8 feet long run the full length on the top plate. One along each side and one down the middle. Four lateral stiffening ribs span the width of the top plate. Two lateral stiffeners are placed 6-inches in from the ends, one in the middle and one on the actuator end. The support end stiffener is 2 feet long and 6-inches

wide. It is mounted on the support end with additional stiffeners to transition from the 6-inch wide end to the 2-inch wide longitudinal stiffeners. All the joints are welded together.

2. Finite Element Analysis and Experimental Correlation

Now that the scale ramp model configuration is set, a finite element model analysis was performed to ensure dynamic responses between the scale ramp model and the full-scale ramp are similar. Initially, the scale ramp model did not match. Lumped masses were added around the model to get the mode shapes and frequencies to match to within an acceptable limit to validate the model.

Once the model was validated, the scale ramp model was manufactured by the mechanical engineering machine shop to the specifications listed in the ramp construction subsection. After construction, the scale ramp model was suspended in a free-free state and a vibration analysis was performed to ensure the actual model dynamic responses matched that of the finite element model. The results of the test are listed in Table 1 and are found to be within acceptable tolerances.

Mode	Mode shape	Scale ramp model frequency (Hz)	Finite element model frequency (Hz)
1	First torsion	10.49	10.74
2	First bending	27.88	25.33
3	Second torsion	43.94	40.50
4	Second bending	79.80	71.16

Table 1. Free-Free Scale Ramp Model Correlation.

B. SUPPORT STRUCTURE

The support structure simulates the RORO attachment point for the scale ramp model. The RORO is so large in comparison to the RRDF that its motion due to RRDF/ramp interaction maybe neglected and assumed fixed. If this assumption proves incorrect, the motion of both the RORO and RRDF may be combined and a single input into the actuator end of the scale ramp model while the other end still remains fixed as in the original assumption. Figure 2 displays two views of the support structure.

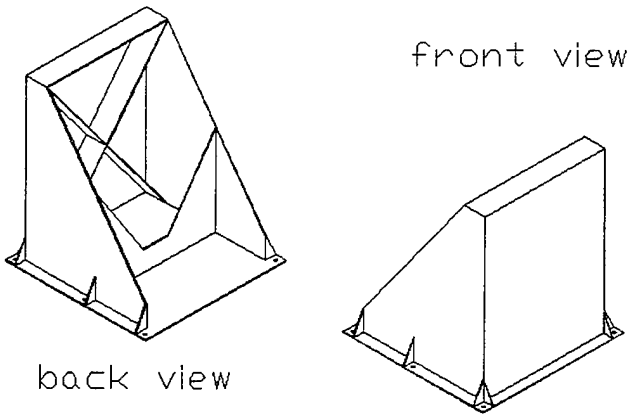

Figure 2. Support Structure.

1. Construction and Fabrication

The support structure is made up of 1/4-inch hot rolled steel plate. The overall dimensions are 42 inches wide by 42 inches deep by 48 inches high. Stiffeners are positioned throughout the structure for reinforcement. All the joints are welded together. Six ¾ inch holes are drilled in the base used for securing the structure to the deck.

2. Finite Element Analysis and Experimental Correlation

A finite element model analysis was performed to ensure dynamic responses of the support structure would not interfere with the scale ramp model testing. The lowest mode of the support structure had a frequency well above the range of frequencies the scale ramp model would be tested at and was deemed a valid structure.

Once the finite element model was validated, the support structure was manufactured by the mechanical engineering machine shop to the specifications listed in the support structure construction subsection. After construction, the support structure was anchored to the deck and a vibration analysis was performed to ensure the support structure dynamic responses matched that of the finite element model. Two of the modes matched very closely. The other mode frequencies, although close were not within an acceptable range and an investigation was conducted to locate the inconsistencies. One cause for the difference was that the joints in the finite element model were complete, full-length welds and the support structure joints, although welded, were not complete, full-length welds. This did not affect the strength of the support structure but did cause testing inconsistencies. The finite element model joints were reconfigured to more closely match those found in the support structure. The second set of results matched more closely but still had some discrepancies. Further evaluation of the support structure

revealed that the plate sizes and placement differed slightly from the finite element model. Continued refinement of the finite element model was suspended. The second set of results were deemed complete and although slightly off, were still well above the range of scale ramp model testing. Results of the final testing of the support structure are listed in Table 2.

Mode	Support Structure frequency (Hz)	Finite element model frequency (Hz)	Mode shape match
1	55.47	51.31	No
2	67.02	71.44	No
3	68.73	72.11	No
4	78.34	93.04	No
5	88.63	96.97	No
6	107.65	102.99	No
7	122.20	119.53	Yes

Table 2. Support Structure Correlation.

C. ACTUATOR

1. Requirements

The requirements are that the free end of the scale ramp model must have the capability to deflect up to twelve-inches peak to peak at a frequency range from zero to 10 hertz. The device that would have to produce this motion must also support a weight of up to 250 lbs. A safety factor (SF) of 2 is utilized in all the design equations. Each

and every design criterion is met well within the required limits indicating the actual safety factor greatly exceeds two in most cases.

Existing shakers that can support the weight constraint did not meet the full twelve-inch travel requirement. Actuators that met the travel constraint could not meet the weight or speed requirements. Finding an actuator that could meet all the constraints started to become very expensive.

The next step was to design an actuator that could meet all the requirements, remain inexpensive and be obtainable in a reasonable amount of time. Some preliminary designs were evaluated and the most suitable design for an actuator was to have a variable speed motor drive an adjustable eccentric mechanism capable the 12-inch peak-to-peak deflection. A connecting rod would transfer the motion from the eccentric mechanism to a carriage, which would travel vertically between linear rails/bearings. The carriage would simulate the RRDF's motion due to wave interaction. Isolation systems would be mounted between the carriage and the scale ramp model for testing. Figure 3 depicts a conceptual drawing of the actuator.

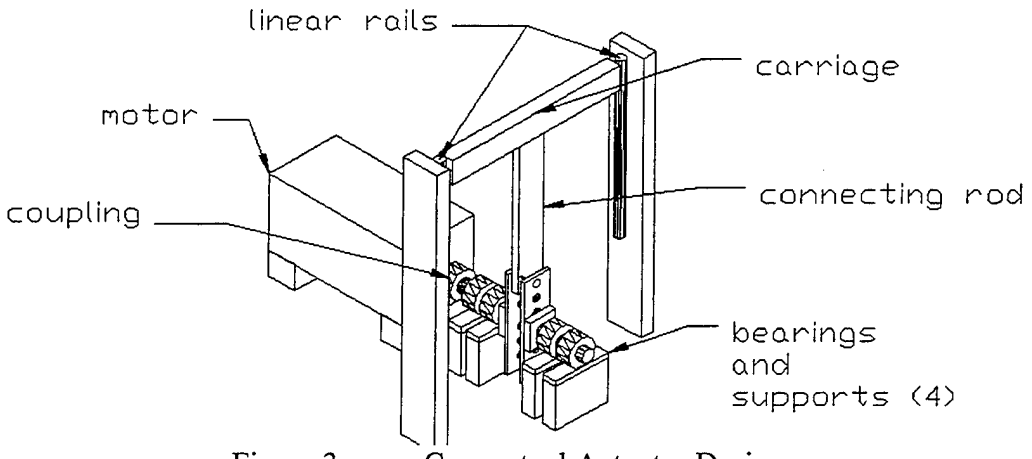

Figure 3. Conceptual Actuator Design.

2. Drive Motor Requirements

The drive motor had to meet certain requirements. One requirement was it had to operate at various speeds so a variable speed motor is needed. First the torque is calculated using the maximum operating parameters the actuator is required to obtain.

$$T = Fd \tag{1}$$

where,
T = torque (ft-lbf)
F = force (lbf)
d = distance (ft)

A torque of 125 ft-lbf is needed using the maximum force of 250 lbs and a distance of one-half foot. Next, the power required is determined.

$$P = T\omega \tag{2}$$

where,
P = power (Hp)
ω = frequency (rads/sec)

10 Hz equates to a frequency of 62.8 rads/sec. This value and the value from Equation (1) are substituted into Equation (2) and give a drive motor power of 14.3 Hp. A motor developing a constant torque with a maximum of 125 ft-lbf, over a speed range of 0 to 600 revolutions per minute (RPM), with a horsepower rating of 15Hp is required. An Allen-Bradley motor is used as the drive motor with the following specifications listed in Table 3.

Horsepower	15 Hp
Input power	460 volts, 60 Hz, 3 phase
Speed	Variable, 650 RPM max
Torque	Constant, (Max125 ft-lbf)
Frame size	L2162
Enclosure	Drip proof, force ventilated

Table 3. Drive Motor Specifications.

3. Drive Shaft Design

The drive shaft couples the motor to the eccentric mechanism. It is supported by two pillow block ball bearings four inches apart and the centerline of the eccentric mechanism is six and one half inches from the end of the last bearing. Keeping the shafts close to the motor shaft diameter and still purchasing an off the self item, a shaft made of 1018 cold drawn (CD) steel with a diameter of one and a half inches was selected. The Ultimate tensile strength (S_{UT}) of the 1018 CD steel is 64,000 pounds per square inch (psi) and the yield strength (S_Y) is 54,000 psi. Figure 4 shows the drive shaft configuration.

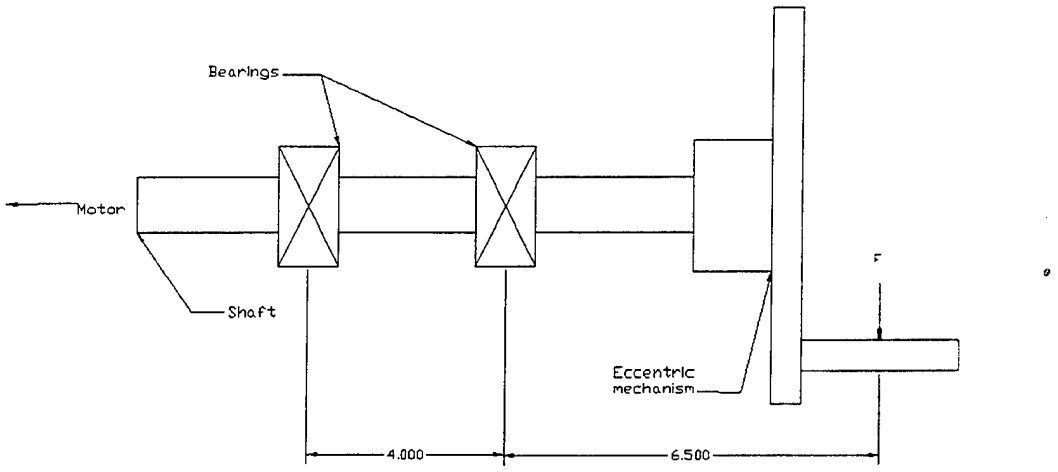

Figure 4. Drive Shaft Configuration.

a. Analysis

The maximum torque applied to the shaft is 1500 in-lbf determined by Equation (1). The moment induced by the maximum weight is 1625 in-lbf as calculated in Equation (3).

$$M = Fa \tag{3}$$

where,
M = moment (in-lbf)
F = force (125 lbf)
a = length (6 1/2 inches)

The applied stress of the shaft based on the Von Mises criteria [Ref. 1] is calculated and must be less than S_Y. A stress of 12,558 psi will be applied to the shaft, which is well below value for S_Y. The shaft will not fail under the static load conditions.

$$\sigma = \frac{32SF}{\pi d^3}\sqrt{M^2 + .75(T^2)} \qquad \leq S_y \tag{4}$$

where,
σ = applied stress (psi)
SF = safety factor (2)
d = shaft diameter (1.5 inches)

Fatigue stress will be calculated based on the Modified Goodman Criteria [Ref. 1]. This criterion states that as long as Equation (5) is less than one, failure will not occur.

$$\frac{\sigma}{S_e}+\frac{\tau\sqrt{3}}{S_{ut}}\leq 1 \tag{5}$$

where,

S_e = corrected endurance limit (psi)

σ = maximum bending stress (psi)

τ = maximum torsion stress (psi)

The corrected endurance limit is determined using Equation (6).

$$S_e = k_a k_b k_c k_d k_e S_e' \tag{6}$$

where,

k_a = surface factor (0.8969)

k_b = size factor (0.833)

k_c = load factor (1)

k_d = temperature factor (1)

k_e = miscellaneous factor (1)

S'_e = endurance limit (psi)

The endurance limit is 32,000 psi as specified in Equation (7).

$$S_e' = \begin{cases} 0.5S_{ut} & S_{ut} \leq 200 \text{ kpsi} \\ 100 \text{ kpsi} & S_{ut} > 200 \text{ kpsi} \end{cases} \tag{7}$$

The maximum bending stress is calculated using Equation (8).

$$\sigma = \frac{M \bullet r \bullet SF}{I} \tag{8}$$

where,

r = shaft radius (in)

I = second moment of area (in^4)

The second moment of area equation is:

$$I=\frac{\pi d^4}{64} \tag{9}$$

where,

d = shaft diameter

The maximum torsion stress is calculated using Equation (10).

$$\tau = \frac{T \bullet r \bullet SF}{J} \tag{10}$$

where,

J = second polar moment of area (in^4)

The second polar moment of area is calculated using Equation (11) .

$$J= \frac{\pi d^4}{32} \tag{11}$$

Solving for Equations (6) through (11) and substituting these values into Equation (5), the modified Goodman criterion gives a value of 0.5329. This is much less than one and the drive shaft will not fail under these fatigue conditions.

4. Idler Shaft Design

The idler shaft helps support the eccentric mechanism and is located on the opposite side of the drive shaft. It is also supported by two pillow block ball bearings four-inches apart with a four-inch span to the eccentric mechanism.

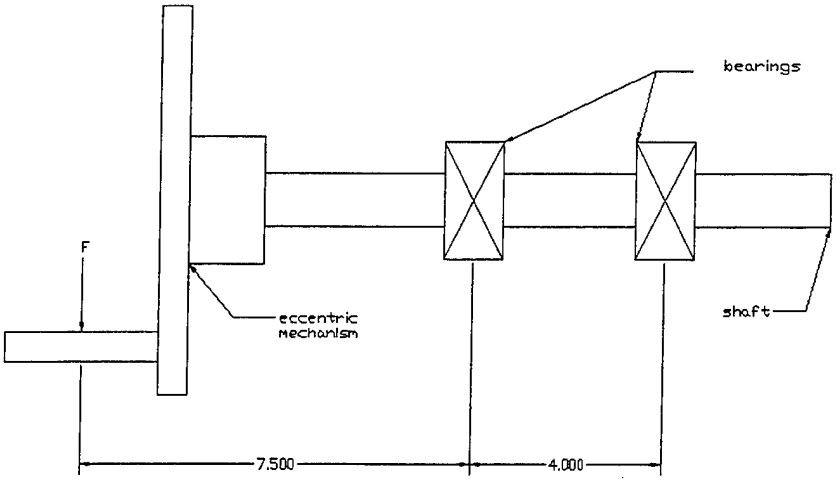

Figure 5. Idler Shaft Configuration.

a. Analysis

The idler shaft analysis utilizes the same equations as the drive shaft. The Modified Goodman criterion gives a value of 0.5961, which is well below the limit of one. However, the value for the idler shaft is larger than that of the drive shaft. This was expected due to the larger span between the bearing and the eccentric mechanism. Still, the idler shaft will not fail under these fatigue conditions.

5. Eccentric Mechanism Design

The eccentric mechanism converts the rotational motion of the motor to a linear motion, which is used to simulate the wave input into the RRDF. Two steel blocks with 1 1/2-inch through holes mount to each shaft. Two steel plates with adjustment holes mount to the blocks, one to each block. The adjustment holes span the plate and vary the peak-to-peak displacement from 2-inches to 12-inches in 2-inch increments. A 1-inch shaft connects the plates to each other. Moving the shaft between the adjusting holes in the plates is how the displacement is varied. One end of a connecting rod is attached to

the eccentric mechanism shaft, the other is attached to the carriage shaft. The carriage rides up and down between a set of linear rails and bearings. This ensures the motion is vertical. Figure 6 depicts the eccentric mechanism configuration.

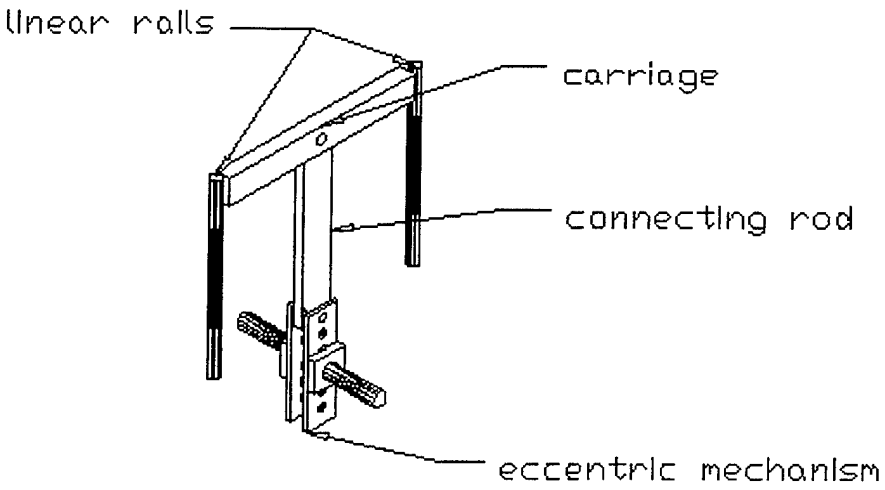

Figure 6. Eccentric Mechanism Configuration.

a. Analysis

The plate is mounted to the block with four 3/8-inch bolts as depicted in Figure 7. The bolts are located 5/8 of an inch from the edges of the block.

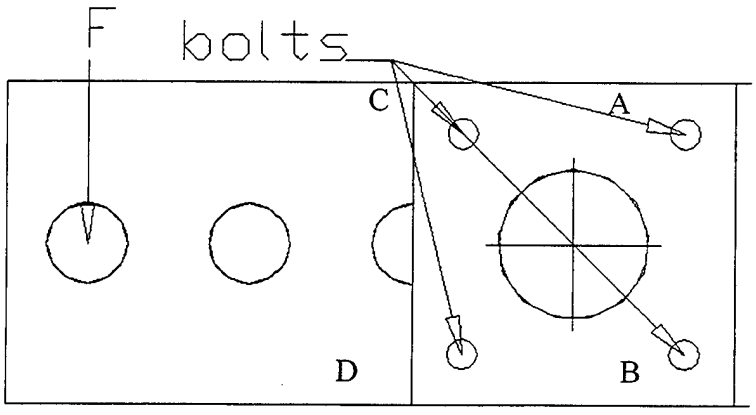

Figure 7. Bolt Shear Diagram.

The grade 2 bolt specifications and material properties are;

bolt minor area (A_r) = 0.0678 in^2

S_{ut} = 74 kpsi,

S_y = 57 kpsi

Using a safety factor of 2 and with the maximum load applied at the maximum deflection adjustment, the stresses on the bolt, plate and block are as follows. A maximum allowable shear (τ_{max}) of 28500 psi is obtained by using Equation (12).

$$\tau_{max} = \frac{1}{2} S_y \tag{12}$$

Due to symmetry, the primary shear load per bolt (F') is 125 lbf as calculated in Equation (13).

$$F' = \frac{F}{n} \tag{13}$$

where,

n = number of bolts (4)

F = maximum load applied (500lbf)

The secondary shear force (F") is 384.6 lbf as calculated in Equation (14).

$$F'' = \frac{M}{4r} \tag{14}$$

where,

M = moment as calculated by Equation (3) with F = 500lbf, a = 6 inches.

r = distance from bolt to centroid of bolt group. (1.95 inches)

The primary and secondary shear forces are added vectorially. Bolts A and B are the critical bolts because they carry the largest shear force of 481.2 lbf each.

These bolts are the limiting factor and will be used for the analysis. As long as bolts A and B meet the design criteria, bolts C and D will also. Using Equation (15), the actual shear stress is calculated to be 7097.2 psi. This is significantly lower than the maximum allowable shear stress of 28500 psi as calculated in Equation (12). The bolts are sufficient to carry the load stated above and will not fail.

$$\tau = \frac{F}{A_r} \tag{15}$$

The bearing stress ($\sigma_{bearing}$) is calculated to ensure the material in the plate will withstand the loading and not have a tensile or shear tear-out. The plate is chosen because it has the smallest thickness and is the critical element. Using Equation (16), the bearing shear stress is 1,283.2 psi. This is well below the acceptable limit and the plate will not fail.

$$\sigma_{bearing} = \frac{F}{A_b} \tag{16}$$

where,

A_b = the bearing area of the plate (0.375 in^2)

(A_b = td, t = plate thickness (1 inch), d = bolt hole diameter (0.375 inches))

The maximum bending stress (σ_b) in the plate is 469.2 psi as calculated using Equation (17). The cross section of the plate at that point is displayed in Figure 8.

$$\sigma_b = \frac{Mc}{I} \tag{17}$$

where,

M=moment as calculated by Equation (3) with F = 500lbf, a = 4 inches

c = distance from the center to the edge of the plate (2 inches)

I = second moment of area of Figure 8. (4.262 in^4)

Equation (18) is the second moment of area for a solid cross-section.

$$I = \frac{bh^3}{12} \tag{18}$$

where,

b = width of cross-section

h = depth of cross-section

Equation (19) is the second moment of area calculation applying the parallel axis theorem for the plate cross-section as depicted in Figure 8.

$$I = \frac{b_1 h_1^3}{12} - \frac{b_2 h_2^3}{12} - \left(\frac{b_3 h_3^3}{12} + Ad^2 \right) \tag{19}$$

where,

b_1 = 1 inch

h_1 = 4 inches

b_2 = 1 inch

h_2 = 1 inch

b_3 = 0.375 inches

h_3 = 1.5 inches

A = 0.5625 inches (area of non-centered cut out)

d = 1.25 inches (distance from the centroid of A to the main centroid)

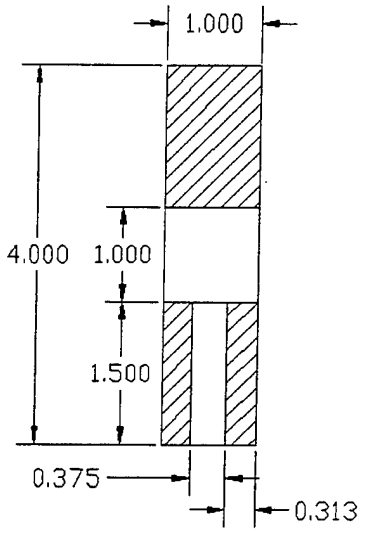

Figure 8. Cross-section of Plate.

6. Carriage Assembly

The carriage assembly plays the role of the RRDF. Figure 9 is the carriage configuration. Located on the ends of the carriage are ball bearing pillow blocks which travel between two vertically mounted linear slide rails. Each ball bearing pillow block is capable of carrying a dynamic load of 1900 lbf. To prevent the carriage from becoming misaligned between the rails, two bearings are placed at each end with a separation of 10 inches.

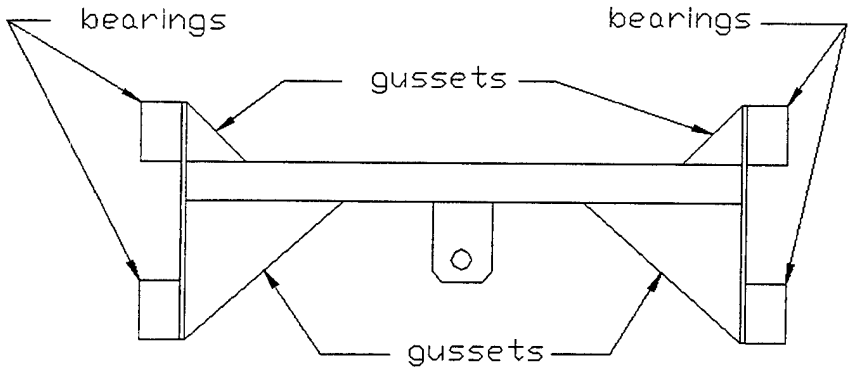

Figure 9. Carriage Configuration.

a. Analysis

The criteria to prevent misalignment is to separate the bearings a specified distance. The minimum separation distance should be greater than or equal to 1/3 the distance of the span between the slide rails. The slide rail separation distance is 28 inches. This gives a minimum bearing separation of 9 1/3 inches. The design meets the criteria and misalignment will not be an issue.

The main body of the carriage is constructed using a 2-inch by 2-inch box beam. Bending stress of the carriage should not be an issue. A cantilever beam evaluation of the carriage beam is used to evaluate the maximum stress encountered. This case produces higher stresses than the actual beam that is fixed at the ends. A stress of 21,000 psi is calculated using Equation (17) with f=500 lbf, c=2 inches and I=1.33 in^3. This is considerably below the allowable stress for the steel beam.

7. Vertical Rail Assemblies

The rails are mounted to 2 inch by 4-inch steel box beams. The beams are welded to a steel foundation plate and reinforced vertically with triangular gussets. A maximum side force of 237.4 lbf applied 20 3/4 inches up from the base plate is developed by the eccentric mechanism transmitted to the box beams via the connecting rod and carriage assembly.

a. Analysis

Applying the force to the top end of the box beam, a stress of 5329 psi is developed using Equation (17) with M=9021lbf-in, c=1 inch, and I=1.693 in^4. This is

lower than the allowable stress for the box beam. Deflection is also an issue so applying the maximum force at the actual point of application, a deflection of 3.2×10^{-5} inches is obtained using Equation (20). This deflection is very small. Adding the reinforcing gussets to the box beam decreases the deflection to an acceptable limit.

$$\delta = \frac{Fl^3}{3EI} \tag{20}$$

where,

l = length from clamped end to point of application. (20.7 inches)

E = Modulus of Elasticity (30×10^6 psi)

7. Connecting Rod

The connecting rod attaches the eccentric mechanism to the carriage assembly. It is fitted with a ball bearing race at each end, which ride on one-inch shafts mounted to the eccentric mechanism and the carriage. The distance between the bearing centers is 14-inches. The connecting rod design is depicted in Figure 10. It carries a compressive load of 553.5 lbf.

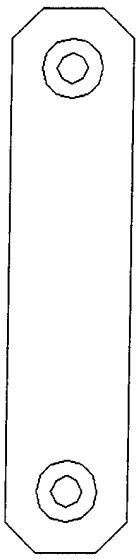

Figure 10. Connecting Rod Design.

a. Analysis

The concern with the connecting rod is buckling since it is only loaded under compression. It has a pinned-pinned connection buckling condition and a fixed-fixed connection buckling condition. Equation (21) is the Euler buckling-load formula.

$$F_{critical} = \frac{\pi^2 EI}{(KL)^2} \tag{21}$$

The pinned-pinned condition gives a critical force of 8.1×10^6 lbf, with $E = 30 \times 10^6$ psi, $I = 5.33$ in^4, and $K = 1$. The fixed-fixed condition, with $I = .33$ in^4 and $K = 0.5$, give a critical force of 2.0×10^6 lbf. The actual force carried is significantly below the critical force in both cases indicating failure due to buckling will not occur.

III. CONCLUSIONS AND RECOMMENDATIONS

The experimental facility to test RORO ramp isolation systems designed in this thesis is a fully operational test platform. All requirements for this facility were fulfilled. A scale ramp model was designed and manufactured. The support structure was designed and manufactured to simulate the RORO. An actuator was designed and manufactured to simulate wave action into the RRDF. The initial calculations used a design safety factor of two. It has been demonstrated that this design met and surpassed the safety factor requirements without concern. Most of the safety factors were well over 5. This may be labeled as over engineered, but it is best to err on the side of caution when delving into new territory.

While designing, manufacturing and evaluating this facility, some recommendations for continued study in this area were identified. Further refinement of the scale ramp finite element model is required to more accurately represent the physical scale ramp model. The support structure finite element model also needs refinement to more accurately represent the physical support and ensure there will not be interference during scale ramp model isolation testing. Design and manufacture new actuator plates for different peak-to-peak displacements other than the ones already provided. Design and manufacture an adjustable interface between the support structure and the scale ramp model for various prototype isolation system heights. Design and manufacture interfaces for mounting the prototype isolation systems between the scale ramp model and the actuator carriage. And finally, obtain the computer software to more accurately control the actuator speed than the current remote control unit.

THIS PAGE INTENTIONALLY LEFT BLANK

LIST OF REFERENCES

1. Shigley, J.E.; Mischke, C.R., *Mechanical Engineering Design*, McGraw-Hill, Inc. 1989

2. Craig, R. R., *Mechanics Of Materials*, John Wiley & Sons, Inc., 1996

3. Lindeburg, M.R., *Mechanical Engineering Reference Manual*, Professional Publications, Inc., 1998

4. Allen-Bradley, 1336 Plus II Adjustable Frequency AC Drive w/ Sensorless Vector, January, 2001

THIS PAGE INTENTIONALLY LEFT BLANK

INITIAL DISTRIBUTION LIST

1. Defense Technical Information Center 2
   8725 John J. Kingman Road, Suite 0944
   Ft. Belvoir, VA 22060-6218

2. Dudley Knox Library 2
   Naval Postgraduate School
   411 Dyer Road
   Monterey, CA 93943-5101

3. Department of Mechanical Engineering 1
   Naval Postgraduate School
   Monterey, CA 93943

4. Naval/Mechanical Engineering Curriculum (Code 34) 1
   Naval Postgraduate School
   700 Dyer Rd., Room 115
   Monterey, CA 93943

5. Professor Joshua H. Gordis, Code ME/GO 1
   Department of Mechanical Engineering
   Naval Postgraduate School
   Monterey, CA 93943

6. Professor Fotis A. Papoulias, Code ME/PA 1
   Department of Mechanical Engineering
   Naval Postgraduate School
   Monterey, CA 93943

7. MR. Jason Chang, Code 282 1
   C/o Commander Carderock Division NSWC
   9500 MacArthur Blvd
   West Bethesda, MD 20817-5700

8. MR. Frank Leban, Code 2820 1
   C/o Commander Carderock Division NSWC
   9500 MacArthur Blvd
   West Bethesda, MD 20817-5700

9. John J McMullen Associates, Inc 1
Edgewood Towne Center Office, Suite 400
1789 South Braddock Ave.
Pittsburgh, PA 15218
Attn: John Chen

10. LT Richard A. Trevisan 1
1317 West Greenfield Ave.
Milwaukee, WI 53204